Int. J. Electrochem. Sci., 7 **(2012)** 2091 - 2108

International Journal of
ELECTROCHEMICAL
SCIENCE
www.electrochemsci.org

Pulse Galvanostatic Synthesis of Zinc-Sulfur Nanocomposites and Application as a Novel Negative Material of Rechargeable Zinc-Manganese Dioxide Alkaline Batteries

Hassan Karami[1,2,*], *Mohammad Ghamooshi-Ramandi*[1]

[1]Department of Chemistry, Payame Noor University, P. O. Box 19395-3697, Tehran, Iran
[2]Nano Research Laboratory, Department of Chemistry, Payame Noor University, Abhar, Iran
[*]E-mail: karami_h@yahoo.com

Received: 22 December 2011 / *Accepted:* 15 February 2012 / *Published:* 1 March 2012

Zinc-sulfur nanocomposite is prepared by using, zinc chloride (0.07 M), and sodium thiosulfate (0.09 M) as precursors in HCl solution with adjusted pH=1 by the pulsed current of 200 mA.cm^{-2} with a frequency of 18 Hz at 0°C. The morphology, the particles sizes, and the composition of each synthesized sample are studied by SEM and XRD. The zinc-sulfur nanocomposite synthesized in optimum conditions includes halo-nanospheres with an average thickness of 50 nm. The sulfur content of the samples is increased when the synthesis temperature is increased. The sample synthesized at 0 °C with low sulfur content (~25%wt) was used as negative (anode) material of rechargeable alkaline zinc-manganese dioxide (RAM) batteries. Some samples are synthesized in the absence of thiosulfate to form nanostructured zinc powder. The performance of zinc-sulfur nanocomposite as negative materials of RAM batteries is compared with those of commercial zinc powder and pure nanostructured zinc powder. The battery tests are shown a discharge capacity 300 mA.h.g^{-1} for zinc-sulfur nanocomposite at first discharges (near to pure nanostructured zinc), but the cycle- life test showed that the zinc-sulfur nanocomposite has a longer cycle-life than the others do.

Keywords: Pulsed current; zinc-sulfur nanocomposite; RAM battery; halo-nanosphere; electrosynthesis

1. INTRODUCTION

Zinc in powder form and metallic cylinder have been used in several types of primary and secondary batteries, such as zinc-manganese dioxide, zinc-polyaniline, zinc-carbon, zinc-air, and zinc-magnesium batteries. The zinc in all of them acts as an anode electroactive material. The zinc-manganese dioxide batteries are characterized as having low cost, ready availability and acceptable performance for a great many applications. These properties include: availability, relatively low price,

environment friendliness, favorable charge density and electrode potential. Today, the excellent shelf -life, high -temperatures service, and environmental friendliness are expected from alkaline Zn/MnO_2 rechargeable batteries, are called RAM batteries. The well-known main problems with the storage and operation of RAM batteries in alkaline media are the corrosion and passivity of zinc anode after some charge-discharge cycles.

Scientific documents show that the major research was focused on the improved MnO_2 ability as a positive material of RAM batteries. Ghaemi et al studied the effects of anodic bath temperature on the electrochemical properties of MnO_2 as the cathode of Ram batteries [1, 2]. They found that the temperature of 120°C is the optimum value to electrochemically produce γ-MnO_2. Ghaemi and Binder showed that a systematic correlation exists between pulse parameters of the electrochemical synthesis of MnO_2 and its ability in RAM batteries [3, 4]. In the other work, Ghaemi et al used electrochemically synthesized MnO_2 in the bipolar system to obtain high discharge capacity and cycle-life for RAM batteries [5]. The effects of different surfactants were studied by Ghaemi et al on the performance of batteries constructed with electrochemically synthesized MnO_2 [6]. Cetyl trimethyl ammonium bromide (CTAB) was shown to have a slight positive effect on the cycle performances of RAM batteries, though sodium *n*-dodecyl benzene sulfonate SDBS inhibits it. Interestingly, the electrochemically synthesized MnO_2 (EMD) powders prepared from the micellar solution, in the range of 0.3 wt% of Triton X-100, exhibited much higher discharge capacities, as well as battery cyclic abilities in comparison with the commercial EMD sample known as TOSOH™. In the previous work, we synthesized manganese dioxide in nanocluster form to improve its capacity and cycle -life [7].

In spite of manganese dioxide, a few reports discuss improving zinc performance as an anode material of RAM batteries. In the 1990s the aqueous $ZnSO_4$ solution was exploited as a replacement for conventional alkaline electrolytes with some promising results [8-10]. The literature data shows that in aqueous $ZnSO_4$ electrolyte discharge and charge reactions of anode (Zn) and cathode (MnO_2) are reversible. On the other hands, some additive materials were used in RAM batteries to improve zinc performance including zinc oxide and magnesium oxide as passivity inhibitors, Carboxy methylcellulose (CMC) as a binder, and acetylene black or graphite powder as a conductive agent [11, 12].

Small metal particles in the nanometer range display chemical and physical properties different from bulk materials. Research interest in the fundamental and functional properties of solid electrodes provides information that can be used to improve the existing technology for further performance enhancement of electroactive materials. Zinc nanoparticles are expected to show improved capacity and cycle -life as an anode of RAM batteries. No reports have been found about the synthesis and application of zinc nanoparticles as anode material in RAM batteries to improve anode performance.

Many reports exit about sulfur nanocomposites as cathodic materials of lithium batteries. Sulfur-polypyrrole [13], sulfur-poly(pyrrole -aniline) [14], sulfur-carbon [15, 16], sulfur-multiwall carbon nanotubes (S/MWCNTs) [17] and sulfur-polyacrylonitrile [18] are examples of sulfur nanocomposites reported as cathode materials. On the other hands, not any report is available about the application of zinc composite or zinc nanocomposite as anode material of batteries.

In this work, we present a new method to synthesize zinc-sulfur nanocomposite. The optimized nanocomposite was used as anode material of RAM batteries and we investigated its discharge capacity and cycle -life.

2. EXPERIMENT

2.1. Materials

All materials and reagents used in this work were of reagent grade and were produced at Loba Chemie Co. (India). Double-distilled water was used in all the experiments.

2.2. Instrumentals

A power source of the MPS-3010L model, made by the Taiwan Matrix Co., was used to produce the constant current. A home-made electrical pulse apparatus was applied to make the reproducible current pulses. The solution temperature was kept constant by the use of a water bath (Optima, Tokyo, Japan).

A scanning electron microscope equipped with EDX instrument from Philips Co. (XL30) was used for the study of morphology, particle size and surface analysis of the prepared iron nanopowders. X-ray diffraction (XRD) studies were performed by a Decker D8 instrument. All battery tests were done by a fully automated battery tester (Batter Test Equipment; BTE 04, Iran).

2.3. Procedure

2.3.1. Synthesis

Reagent- grade zinc chloride and sodium thiosulfate were used as the precursors. The appropriate amounts of zinc chloride (0.07 M) and sodium thiosulfate (0.09 M) were dissolved in hydrochloric acid (pH = 1). The obtained solution was used in the electrochemical synthesis cell with two coaxial cylindrical platinum grid electrodes as anode and cathode. The 200 $mA.cm^{-2}$ pulsed current with 18 Hz frequency and 14 ms pulse time was applied for 2 h. After electrosynthesis, the obtained precipitate of zinc-sulfur nanocomposie was filtrated from the solution and washed with water and ethanol. Lastly, washed yield was sonicated in ethanol for 1 h to obtain uniform nanostructures without any agglomerating or other physical adhesions. The sonicated nanocomposite was dried at room temperature. The morphology, dimension size, and structure of zinc-sulfur nanocomposite powder were studied by SEM and XRD.

By use of this method, some effective parameters occur that include pulse amplitude (current amount or pulse height), pulse frequency, zinc chloride and sodium thiosulfate concentrations, solution pH, and temperature of synthesis solution, which were optimized by the "one at a time" method.

2.3.2. Battery construction and tests

The optimized zinc-sulfur nanocomposite was used as anode material for the construction of laboratory scale zinc-manganese dioxide batteries. Two other anode materials including pure nanostructured zinc powder and industrial zinc powder (which is used in the manufacture of RAM batteries) were used to compare the anode ability of synthesized nanocomposite. The battery scheme was shown in Fig. 1. We then mixed 0.1 g zinc-sulfur nanocomposite powder was mixed with 9 %wt KOH solution to obtain a anodic paste. The resulting paste was soft- pressed in the anode hole of the battery. Industrial zinc powder and nanostructured zinc powder were mixed with 1 %wt CMC, 2 %wt MgO, 4 %wt ZnO and 1 %wt acetylene black. The obtained 0.1 g blend was mixed with KOH 9 %wt to form a hard paste. The paste was soft pressed in the anode hole of the battery plan.

We mixed 0.27 g industrial manganese dioxide (RAM battery grade) with 0.03 g of acetylene black, then with 9 %wt KOH solution. The cathode paste was soft pressed into the cathode hole of the laboratory designed- batteries (Fig. 1).

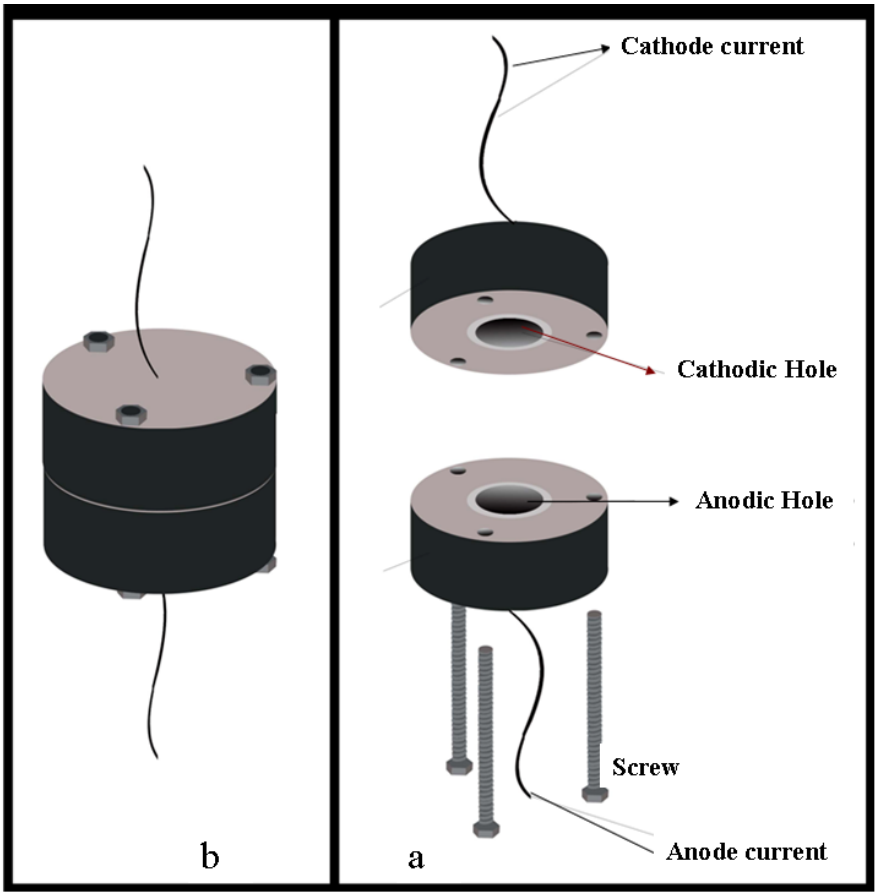

Figure 1. Scheme of the designed battery plan

The weight of cathodic electroactive material was more than of anode material; therefore the anode material is the limiting factor to control battery performance. Discharge capacities and the

performances of the consecutive charge/discharge cycles of the zinc-sulfur nanocomposite, the pure zinc nanopowder and the conventional zinc powder were measured as the main anodic component of the laboratory designed RAM batteries. All cells have been discharged galvanostatically at a current density of 22.5 mA (225 mA.h.g^{-1} anode material) to reach a cut-off voltage of 1.0 V. A charge process was also done by 225 mA.h.g^{-1} constant current for 2 h. Each test was repeated at least two times with similar results and the reproducibility of the data was confirmed.

3. RESULTS AND DISCUSSION

In this procedure, zinc-sulfur nanocomposites were produced by exerting electrochemical pulses into a solution containing two platinum cylindrical grid electrodes. Experimental observations showed that the synthesized zinc-sulfur nanocomposites do not stick to the electrode surface in this method. The synthesized particles immediately leave the electrode surface and disperse into the solution. Therefore, the electrode surface is not completely covered by the synthesized particles. In this method, there are some effective parameters that include pulse amplitude (current amount or pulse height), pulse frequency, zinc chloride and sodium thiosulfate concentrations, solution pH, and temperature of synthesis solution which were optimized by the "one at a time" method. To obtain a sample with suitable morphology, particles sizes, and composition, we carried out several experiments, and their conditions are summari zed in Table 1.

In this work, we learn from our previous experiences regarding the pulsed- current method. Those studies had shown that the pulsed- current method is more effective than the simple constant voltage and simple constant current methods [19-21] for the synthesis of nanomaterials. The pulsed-current electrochemical method can be used as a confident and controllable method for the production of nanoparticles. This pulsed- current method has 4 variable parameters: pulse height (current amplitude), pulse time, relaxation time, and pulse frequency. Our initial studies showed that the relaxation time/pulse time ratio of 3 is a suitable value to obtain a suitable synthesis. Thus, the ratio of 3 was selected for further studies. At a constant ratio of relaxation time to pulse time, a pulsed current has 3 variable parameters: pulse height, pulse time, and pulse frequency. Each current pulse contains a "t_{on}" time (pulse time) and a "t_{off}" time (relaxation time) so that the pulse frequency can be related to the sum of current pulses, which can be applied in to the system in one second. At a constant ratio of relaxation time/pulse time (ratio = 3), any variation in pulse frequency creates new pulse and relaxation times.

The pulse time and pulse frequency are two dependent parameters. The pulse time is decreased as the pulse frequency is increased and can be calculated from equation 1:

$$t_{on} = \frac{1}{f} \times K \times 1000 \qquad \text{(eq. 1)}$$

In this equation, t_{on}, f, and K are pulse time in ms, pulse frequency in Hz, and pulse ratio (ratio of pulse time to relaxation time), respectively. For example, when pulse frequency is 18 Hz,

t_{on} will be 14 ms. With respect to the above equation, in the optimization process pulse time will be optimized when the pulse frequency is optimized (without any other step).

Table 1. Synthesis conditions of optimization experiments

Pulse height ($mA.cm^{-2}$)	Sodium thiosulfate concentration (M)	Zinc nitrate (M)	pH	Pulse frequency (Hz)	Temperature (° C)
100	0.09	0.07	0	9	75
100	0.09	0.07	1	9	75
100	0.09	0.07	2	9	75
100	0.09	0.07	3	9	75
100	0.09	0.07	4	9	75
100	0.09	0.07	1	0	75
100	0.09	0.07	1	6	75
100	0.09	0.07	1	9	75
100	0.09	0.07	1	12	75
100	0.09	0.07	1	15	75
100	0.09	0.07	1	18	75
100	0.09	0.07	1	21	75
100	0.09	0.07	1	24	75
100	0.09	0.07	1	18	75
30	0.09	0.07	1	18	75
70	0.09	0.07	1	18	75
100	0.09	0.07	1	18	75
150	0.09	0.07	1	18	75
200	0.09	0.07	1	18	75
250	0.09	0.07	1	18	75
200	0.02	0.07	1	18	75
200	0.05	0.07	1	18	75
200	0.07	0.07	1	18	75
200	0.09	0.07	1	18	75
200	0.12	0.07	1	18	75
200	0.2	0.07	1	18	75
200	0.09	0.01	1	18	75
200	0.09	0.02	1	18	75
200	0.09	0.05	1	18	75
200	0.09	0.07	1	18	75
200	0.09	0.1	1	18	75
200	**0.09**	**0.07**	**1**	**18**	**0**
200	0.09	0.07	1	18	25
200	0.09	0.07	1	18	50
200	0.09	0.07	1	18	75
200	0.09	0.07	1	18	100

When pulse current is exerted into the cell, two cathodic reactions can be carried out as follow:

eq. (2) $$Zn^{2+} + 2e \rightarrow Zn$$

eq. (3) $$S_2O_3^{2-} + 6H^+ + 4e \rightarrow 2S + 3H_2O$$

The amount of each reaction depends on zinc ion concentration, thiosulfate ion concentration, pH, and temperature. Pure zinc powder can be synthesized in the absence of sodium thiosulfate. The effects of each parameter will be changed to obtain suitable morphology, smaller particles and suitable composition for zinc-sulfur nanocomposites.

3.1. pH effect

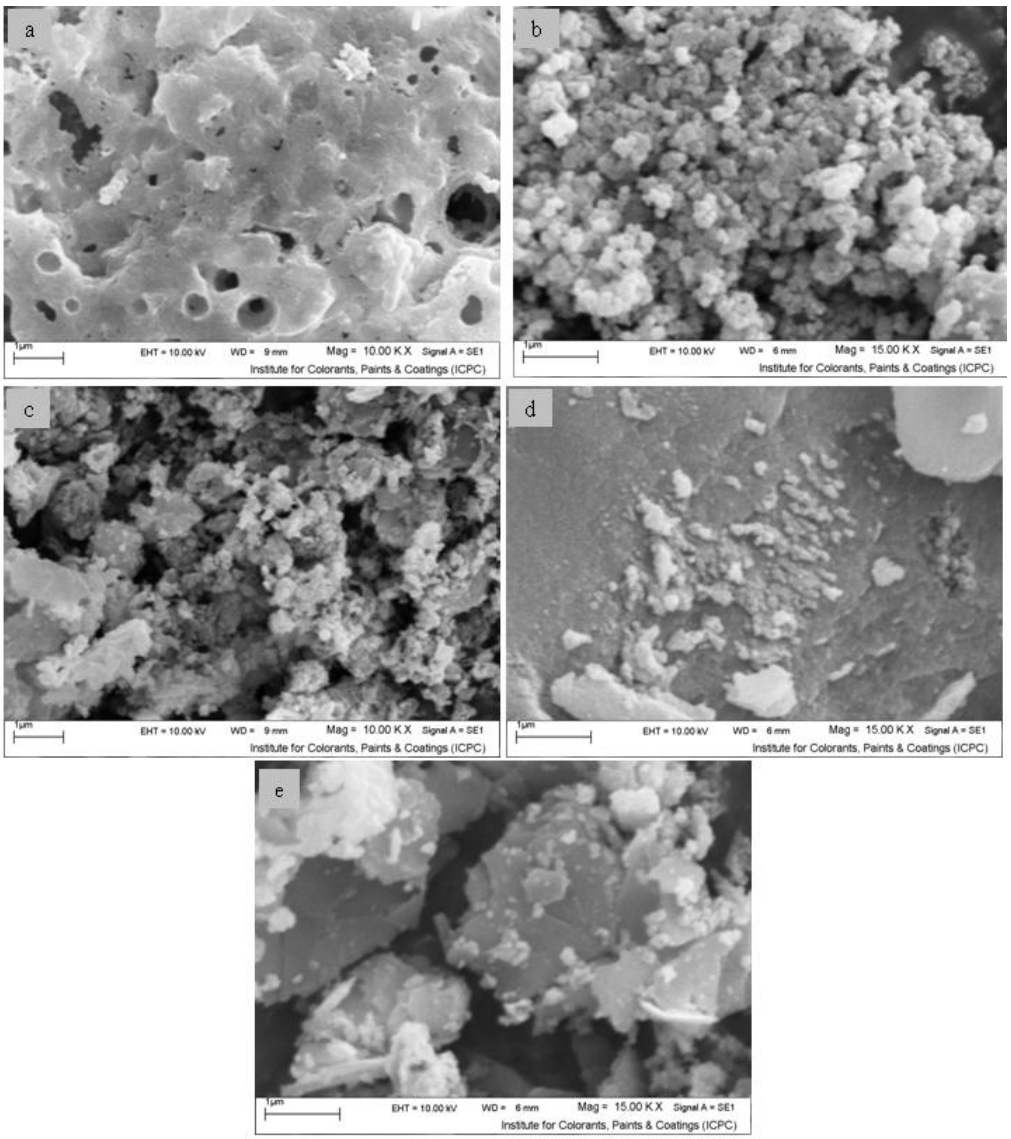

Figure 2. SEM images of the samples synthesized at different pH of initial solutions: (a) 0, (b) 1, (c) 2, (d) 3, and (e) 4.

Based on eq. 3, the synthesis of zinc-sulfur nanocomposites is strongly depend on solution pH, so this parameter was varied from 0 to 10. At pH 5 and more, zinc ions precipitate as zinc hydroxide. Zinc-sulfur nanocomposites were synthesized at pH range of 0 to 4. Figure 2 shows the SEM images of the samples synthesized at different pH's.

We can see in Fig. 2 that, the pH of 1 is a suitable amount to synthesize a powder including more- uniform nanostructures. The use of higher pH's cause decrease uniformity of the sample morphology and also increase particles sizes. The results of XRD analyses of the samples are summarized in Fig. 3.

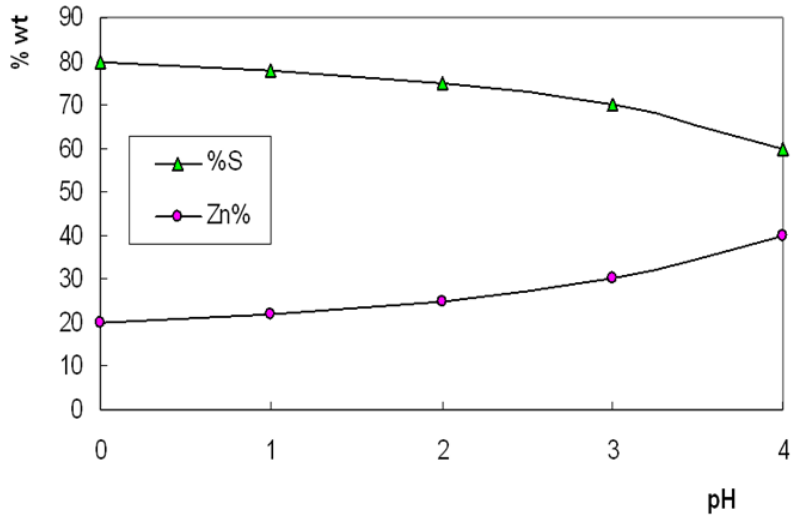

Figure 3. Phase composition analysis of the samples synthesized at different solution pHs.

As it can be seen in Fig. 3, use of lower pHs cause decrease the zinc content and increase the sulfur content of the samples. Phase composition analysis of the samples showed that the sulfur content was decreased from 80 %wt at pH 0 to 60 %wt at pH 4. On the other hand, the zinc content of the samples changes by any variation in the pH of the initial synthesis solution exactly opposite of the sulfur content. Based on the sulfur content and specially the sample morphology, the pH value of 1 was finally selected for our next experiments.

3.2. Pulse frequency

Dc current pulse is an electron package that can be exerted into the electrochemical cell during a specific time (pulse time) to make a reaction. Each electron package contains many electrons that cause oxidation and reduction of some anodic and cathodic species, respectively. In this work, one zinc-sulfur nanocomposite will be formed when an electron pulse passes from the cell. When the pulse frequency is increased, the electron package sizes will be smaller, but the number of pulses per second will be increased. It is expected that the morphology and the particles sizes of the samples strongly depend on the pulse frequency. To get an experimental conclusion, eight syntheses were carried out at

different pulse frequencies to investigate the effect of this parameter on the morphology and particles sizes of the samples. Figure 4 shows the SEM images of the samples synthesized at different pulse frequencies. When the pulse frequency changes, the number of electrons in each pulse (they are used in synthesis) is changed so that the mechanism, particle growth, and agglomeration rates of the final product.

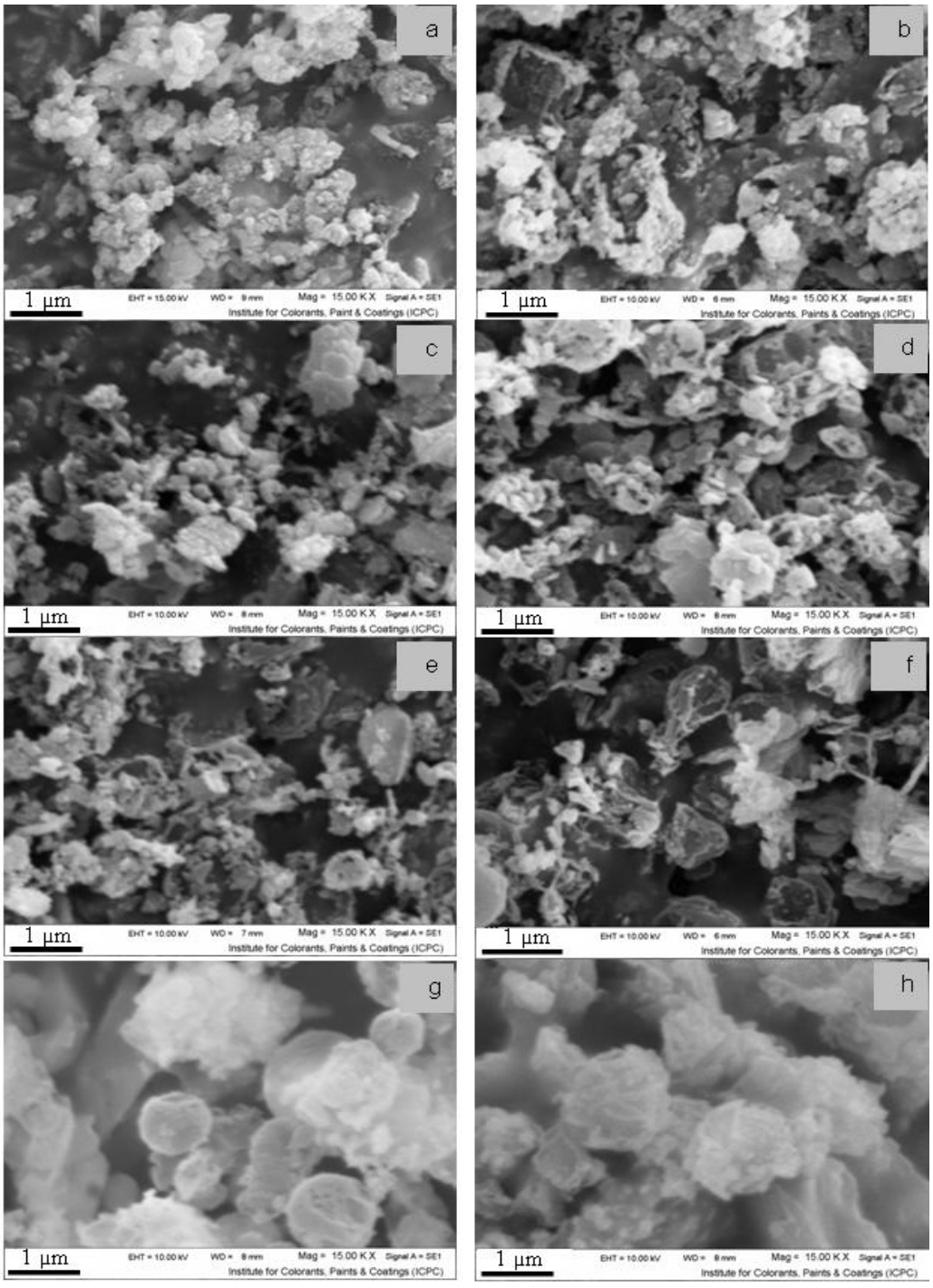

Figure 4. SEM images of the samples synthesized at different pulse frequencies: (a) without pulse, (b) 6 Hz, (c) 9 Hz, (d) 12 Hz, (e) 15 Hz, (f) 18 Hz, (g) 21 Hz, and (h) 24 Hz.

As Fig. 4 shows, the pulse frequency is a strong parameter that can affect on the morphology and the particles sizes of the zinc-sulfur nanocomposite. The uniformity of the samples is increased by increasing pulse frequency to 24 Hz. Nanoscale semi-spheres are seen at pulse frequency range of 15 to 21 Hz. At the pulse frequency 24 Hz, nanoscale semi-spheres are converted to the non-uniform particles. Applying the synthesis current in pulse form decreases the nuclear growth and also controls the mechanism of product formation; thus the uniform nanospheres in powder form are synthesized. Figure 4 shows that the frequency of 18 Hz is a suitable amount to synthesize a powder including more- uniform nanostructures.

3.3. Pulse height

To investigate the effect of pulse current amplitude (pulse height or current density) on the morphology and particles sizes, the pulse height varied from 10 to 250 mA.cm^{-2}, but the other parameters were kept constant (see Table 1). Figure 5 shows the effect of pulse height on the morphology and size of yield zinc-sulfur nanocomposites.

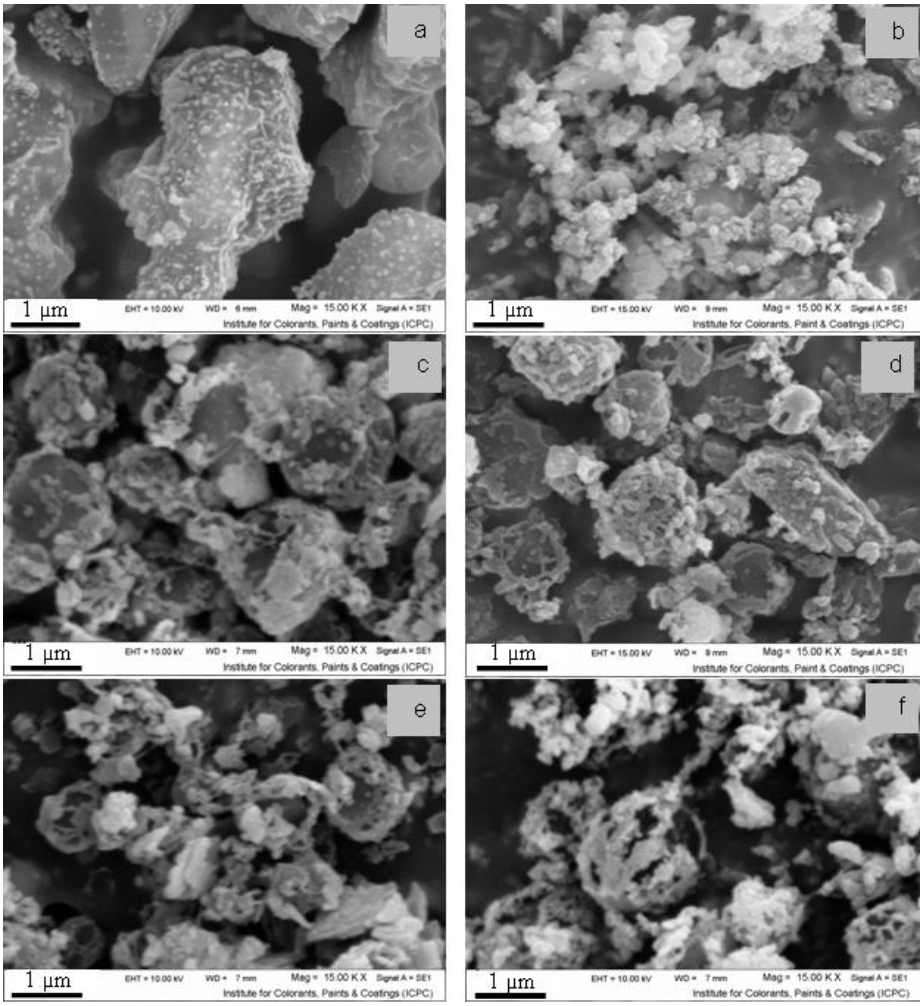

Figure 5. Effects of pulse height (current density) on the morphology and particle size of samples: (a) 10, (b) 50, (c) 100, (d) 150, (e) 200, and (f) 250 mA cm^{-2}.

As shown in Fig. 5, the 200 mA.cm-2 current density is a suitable amount to synthesize a powder that includes more- uniform nanostructures. Exerting higher currents causes increase the cell voltage. High cell voltage makes non-selective redox reactions so that this phenomenon makes non-homogeneous morphology and larger particles. The obtained results are comfortable with the previous report [19]. At lower current density (10 mA cm-2), particle growth rate is greater than the nucleation rate; thus a sample is obtained with larger particles.

3.4. Thiosulfate ion concentration

To investigate the effects of thiosulfate ion concentration, this parameter was varied from 0.02 to 0.2 M (samples 21 to 26). The SEM images of the synthesized samples were shown in Fig. 6.

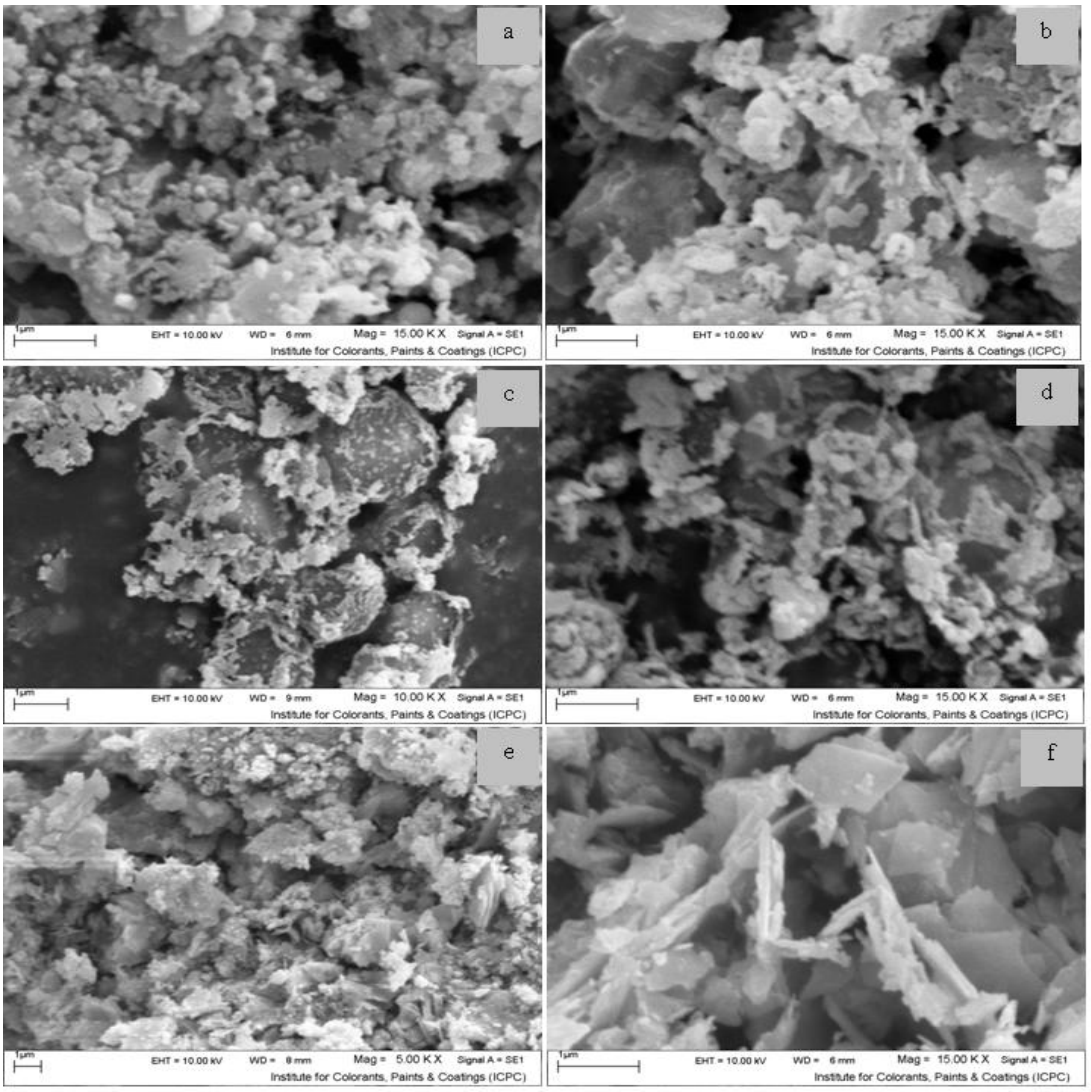

Figure 6. SEM images of the samples that synthesized at different concentrations of sodium thiosulfate: (a) 0.02, (b) 0.05, (c) 0.07, (d) 0.09, (e) 0.12, and (f) 0.2 M.

As Fig. 6 shows, the thiosulfate concentration is an important parameter in the presented

synthesis. The reactions 2 and 3 show the thiosulfate concentration can acts as a main factor in the kinetic equation of the synthesis. It is obvious that the amounts of kinetic equation factors make considerable changes in synthesis rate and consequent on the morphology and particles sizes of the samples. On the other hand, the reactions 2 and 3, shows that the thiosulfate concentration can change the nanocomposite composition. Therefore the samples 21, 24, and 26 (Table 1) were analyzed by XRD. Table 2 shows the ingredients of three samples synthesized at different concentrations of thiosulfate (extracted from XRD patterns).

Table 2. Sulfur content of Zn-sulfur nanocomposites synthesized at different thiosulfate concentrations

Thiosulfate concentration (M)		0.02	0.09	0.2
Sample composition	Zn (%wt)	40	23	10
	Sulfur (%wt)	60	77	80
	Zinc Sulfide (%wt)	0	0	10

Based on the obtained results, the thiosulfate concentration directly controls the sulfur content of the nanocomposite. Based the XRD and SEM results, 0.09 M was selected as a suitable concentration for sodium thiosulfate. In this concentration, the sample had not only suitable morphology, but also suitable composition. In concentrations of less than 0.02 M, the amount of the product is very small. Therefore, the sample synthesized at lower concentrations of thiosulfate can not be filtrated and collected.

3.5. Zinc chloride concentration

In this step, zinc chloride concentration varied from 0.01 to 0.1 M, though the other parameters were kept constant. Each obtained sample was studied by SEM to investigate morphology and particles sizes (Fig. 7). As Fig. 7 shows, the nano-semi-spheres in the lowest concentration (0.01 M) is converted to the nanospheres in 0.07 M. This phenomenon can be related to the kinetic and mechanism of zinc/sulfur nanocomposite formation being strongly depends on the zinc ion concentration. Because of higher synthesis rate at higher concentrations (more than 0.07 M), uniformity of the samples is decreased and particle growth is increased.

Based on the obtained results, many uniform nanospheres of zinc/sulfur nanocomposite can be synthesized at 0.07 M zinc chloride.

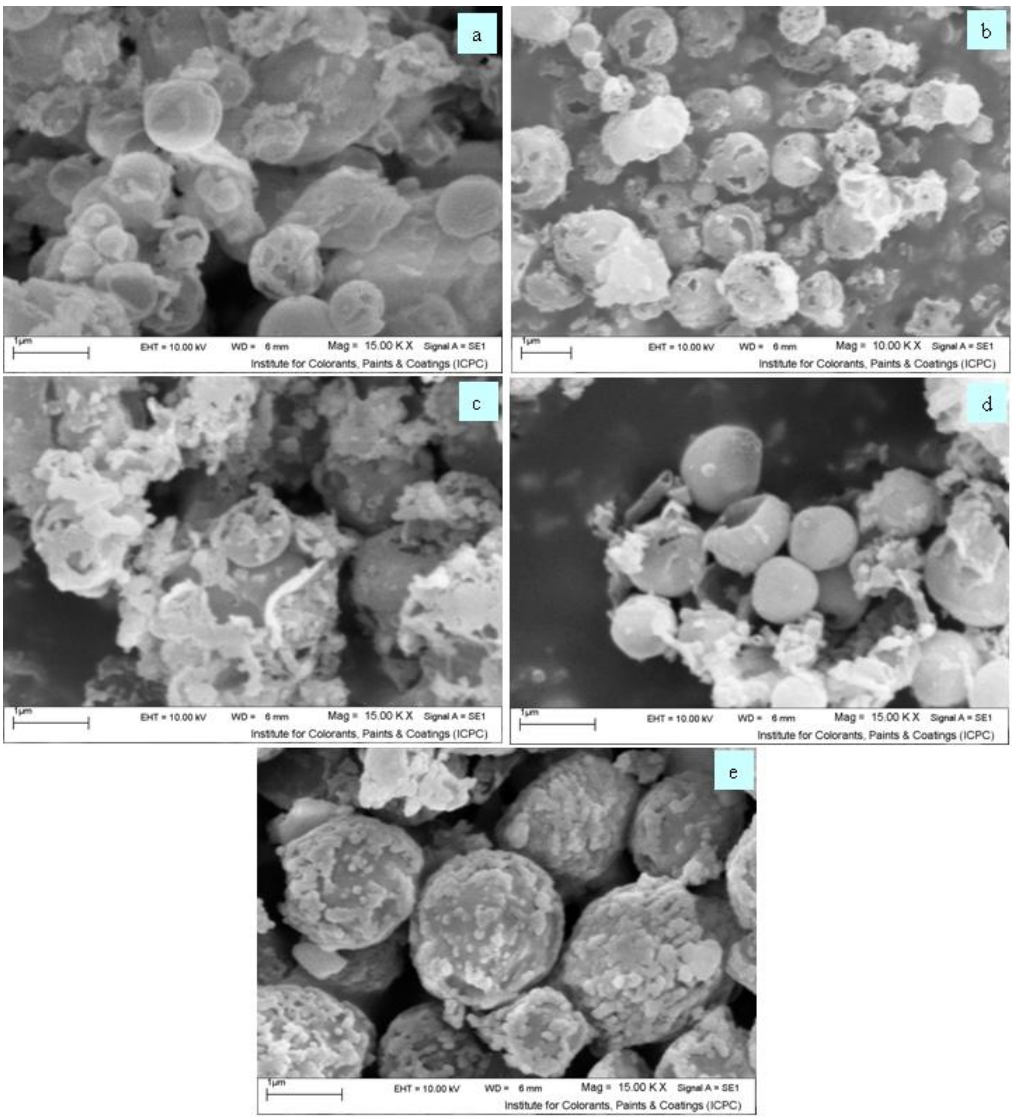

Figure 7. SEM images of the samples which synthesized at different concentrations of zinc chloride: (a) 0.01, (b) 0.02, (c) 0.05, (d) 0.07, (e) 0.1 M.

3.6. Effects of synthesis temperature

To investigate the effect of synthesis temperature on the morphology, particles sizes, and composition of the samples, seven syntheses were carried out at different temperatures: 0, 25, 50, 75 and 95ºC. Figure 8 shows the XRD patterns of the samples synthesized at these temperatures. Based on XRD patterns, the Zn content of the samples is decreased when the synthesis temperature is increased (Fig. 9). XRD patters of the samples (Fig. 8) showed that there is not any impurity of ZnS in the synthesized samples. The rate of reaction 3 (eq. 3) increases more than the rate of reaction 2 (eq. 2) when the synthesis temperature is increased.

Figure 10 shows the SEM image of the optimum sample (sample 32, Table 1). The optimized zinc/sulfur nanocomposite includes halo-nanospheres with an average diameter of 500 nm and an average thickness of 50 nm.

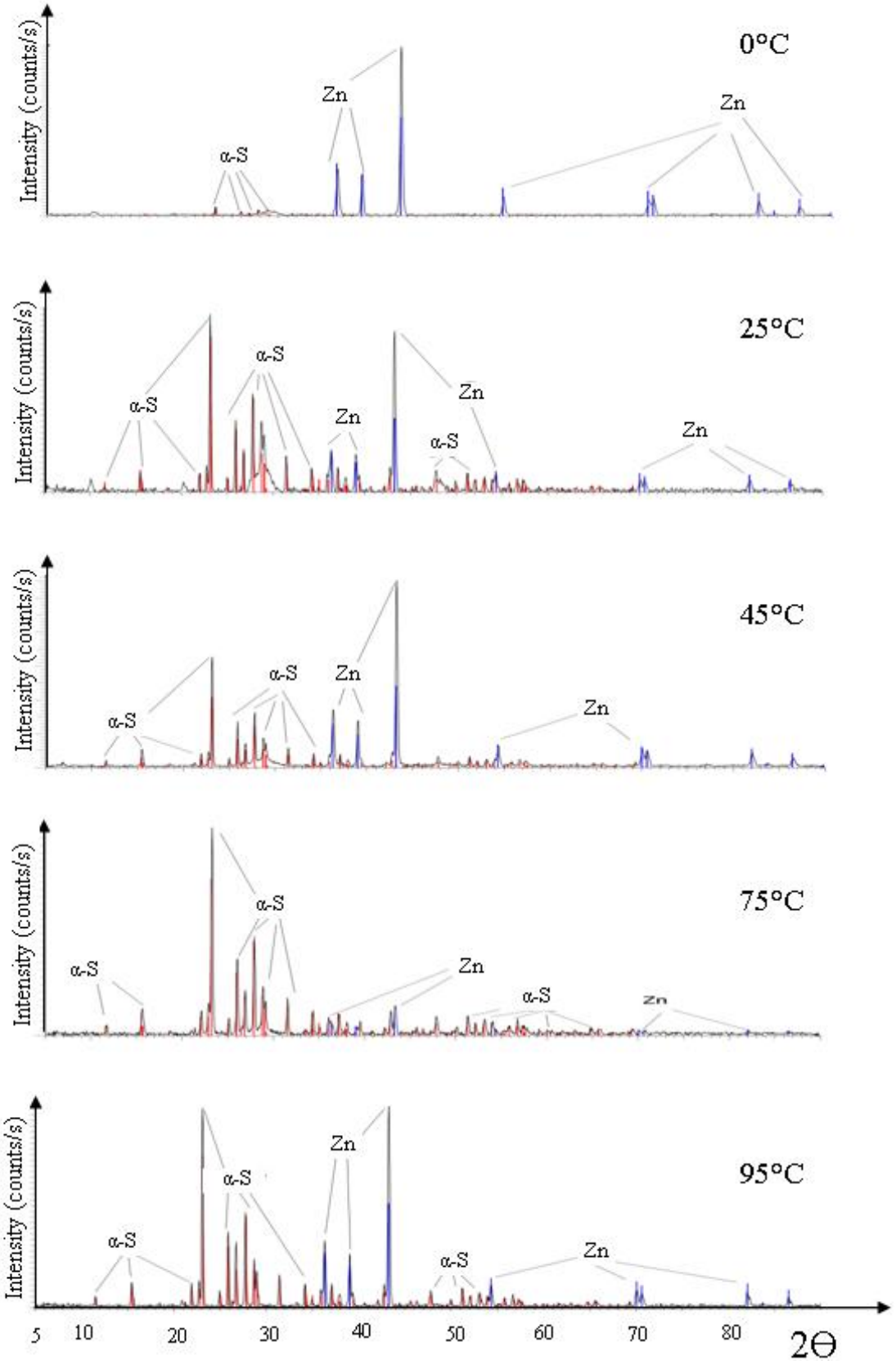

Figure 8. XRD patterns for the samples that synthesized at different solution temperatures: (a) 0^{O}C, (b) 25^{O}C, (c) 50^{O}C, (d) 75^{O}C, and (g) 95^{O}C.

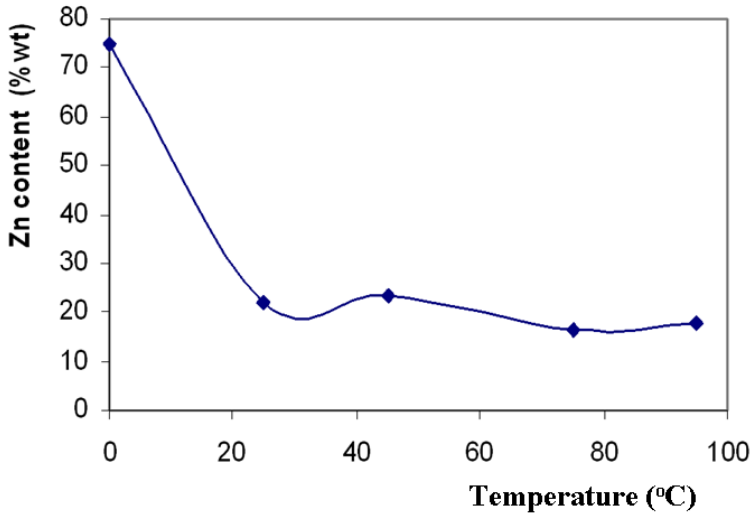

Figure 9. Effects of synthesis temperature on the zinc content of samples

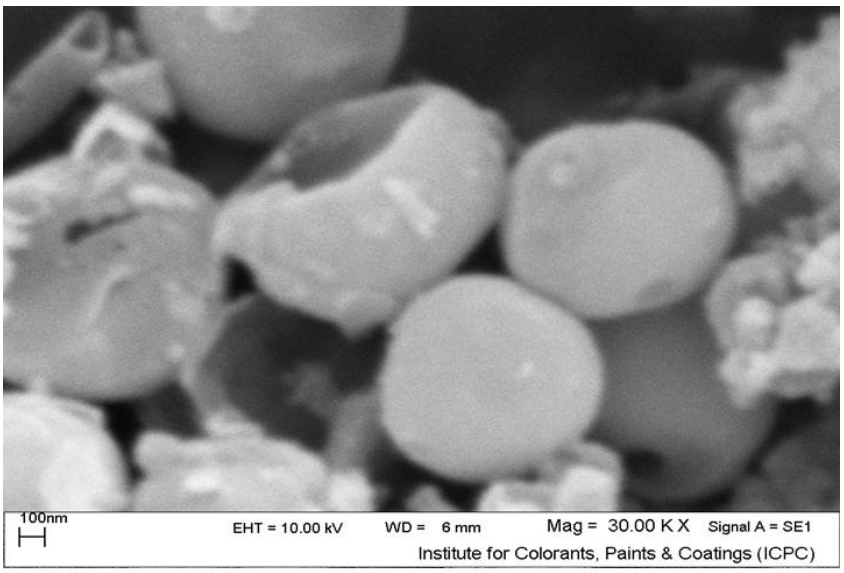

Figure 10. SEM image of the sample synthesized in optimum conditions (pH = 1, pulse frequency 18 Hz, pulse height 200 $mA.cm^{-2}$, sodium thiosulfate 0.09 M, zinc chloride 0.07 M, and synthesis temperature $0^{O}C$).

3.7. Battery laboratory tests

For an evaluation of the zinc-sulfur nanocomposite including nanospheres with 25% sulfur content as the anode of RAM batteries, its discharge capacity and cycle- life were determined and compared to those of pure nanostructured zinc powder and conventional anodic powder of RAM batteries. Figure 11 shows the time-voltage behaviors of three RAM batteries constructed by three different anodes, conventional zinc powder, pure zinc nanopowder and zinc-sulfur nanocomposite. It

should be mentioned that each curve in Fig. 11 is the average curve for three consecutive discharge cycles.

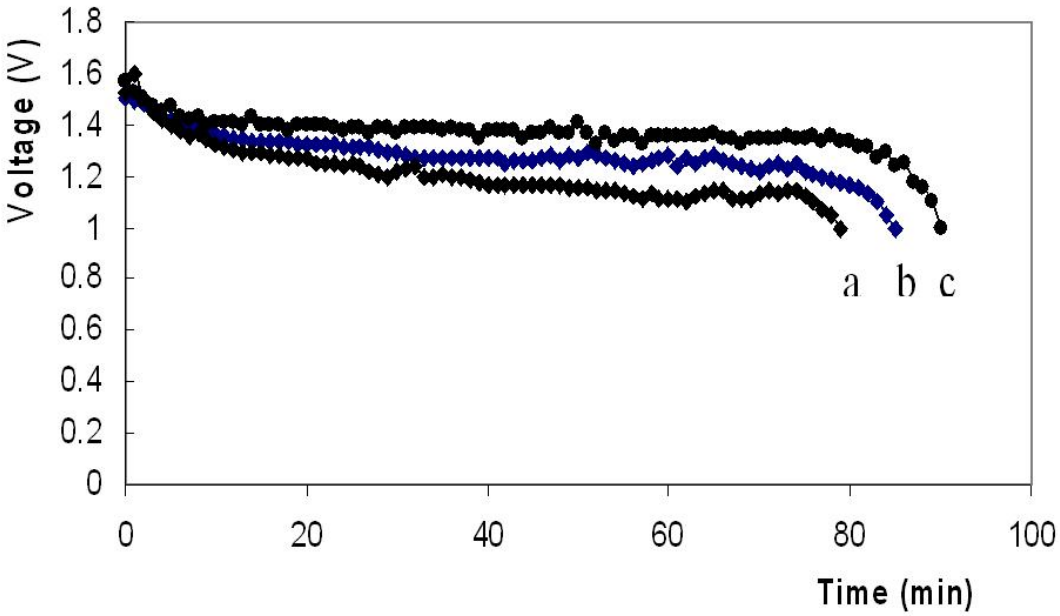

Figure 11. Time-voltage behaviors of three batteries constructed with different anodic materials during discharge under constant current, including (a) nanocomposite, (b) conventional zinc powder, and (c) zinc nanopowder.

As Fig. 11 shows, the discharge capacities of 326, 312 and 300 mA.h.g-1 were obtained with respect to weight of zinc powder used in anode construction for pure zinc nanoparticles, conventional zinc powder, and zinc-sulfur nanocomposite, respectively. Based on these results, zinc-sulfur nanocomposite is not a good candidate for the anodic material of RAM batteries. The low discharge capacity of the nanocomposite can be related to this fact that the anodes constructed with pure zinc nanoparticles and conventional zinc powder include some additives (ZnO, MgO, CMC, and acetylene black as noted in section 2.3.2). However, the nanocomposite was used without any additive.

To get a trust conclusion, three cycle-life tests using the same method were performed on three types of batteries (section 2.3.2). Figure 12 shows the cycle-life curves for the three constructed batteries. In Fig. 12, the zinc-sulfur nanocomposite has obviously less loss of discharge capacity than the others, thus it has a longer cycle- life. Discharge capacities after 50 cycles for the commercial powder, pure zinc nanopowder and the zinc-sulfur nanocomposite were 70, 140 and 160 $mA.h.g^{-1}$, respectively. The long cycle- life for the nanocomposite is due to the sulfur molecules (S8) acting probably as a cross- linker (transverse bridge agent) between zinc atoms during consecutive charge/discharge processes. This phenomenon causes the connection to remain always established between the zinc atoms. The stable connection between zinc atoms prevents any decrease in the discharge capacity. On the other hands, sulfur molecules probably prevent any forming passive species in anode paste. The final result of sulfur presence in the nanocomposite is to prevent capacity loss.

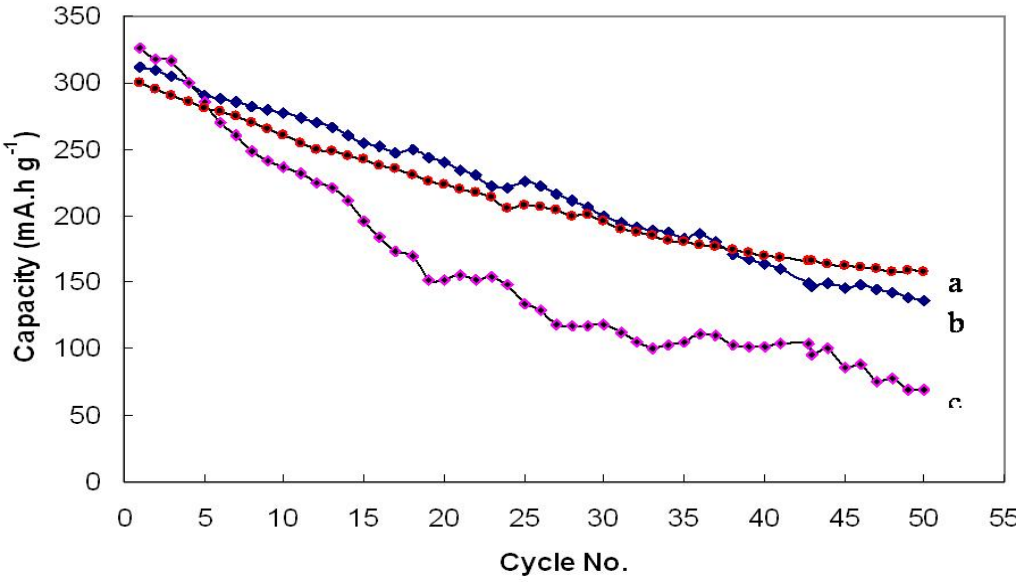

Figure 12. Variations of discharge capacities during 50 consecutive cycles for three batteries constructed with different anodic materials including, (a) nanocomposite, (b) zinc nanopowder, and (c) conventional zinc powder.

To find some information about the formation of ZnS during charge/discharge cycles, the anodic material of the constructed battery was analyzed by XRD after 50 charge/discharge cycles. The obtained patterns were very similar to Fig. 8b. The obtained XRD patterns also include minor ZnO impurity. Formation of ZnO in rechargeable alkaline Zn-MnO2 batteries has previously reported. Electroactivity of sulfur can make some species such as sulfide, sulfate, thiosulfate and similar compounds during consecutive charge/discharge cycles. Based on the XRD patterns, there was not any similar impurity. This fact shows that sulfur content of the nanocomposite doesn't have electroactivity.

4. CONCLUSION

The obtained results in this work indicate that the pulsed- current electrochemical method can be used as a confident and controllable method to synthesize zinc/sulfur nanocomposites. When a synthesis is carried out under conditions that include 18 Hz pulse frequency, 200 $mA.cm^{-2}$ pulse height (current amplitude), 0°C synthesis solution temperature, 0.07 M zinc chloride, and 0.09 M sodium thiosulfate in hydrochloric acid solution with pH of 1, the nanocomposite of zinc/sulfur in nanosphere form can be obtained. The synthesized nanocomposite can be used as anodic material of RAM batteries with long cycle- life.

ACKNOWLEDGEMENTS
We gratefully acknowledge the support of Abhar Payame Noor University Research Council throughout these research experiments.

References

1. M. Ghaemi, Z. Biglari, and L. Binder, *J. Power Sources* 102 (2001) 29.
2. M. Ghaemi, R. K. Ghavami, L. Khosravi-Fard, and M. Z. Kassaee, *J. Power Sources* 125 (20040 256.
3. M. Ghaemi and L. Binder, *J. Power Sources* 111 (2001) 248.
4. H. Adelkhani and M. Ghaemi, *Solid State Ion*. 179 (2008) 2278.
5. M. Ghaemi, R. Amrollahi, F. Ataherian, and M. Z. Kassaee, *J. Power Sources* 117 (2003) 233.
6. M. Ghaemi, L. Khosravi-Fard, and J. Neshati, *J. Power Sources* 141 (2005) 340.
7. H. Karami, M. Ghamooshi-Ramandi, S. Moeini and F. Salehi, *J. Clust. Sci*. 21 (2010) 21.
8. T. Yamamoto, T. Shoji, *Inorg. Chimica Acta* L27(1986) 117.
9. T. Shoji, M. Hishinuma, T. Yamamoto, *J. Appl. Electrochem*. 18 (1988) 521.
10. S. Kim, Patent US 6187475.
11. H. Karami, M. F. Mousavi and M. Shamsipour, *J. Power Sources* 117 (2003) 255.
12. H. Karami, M. F. Mousavi, M. Shamsipour and S. Riahi, *J. Power Sources* 154 (2006) 298.
13. X. Liang, Y. Liu, Z. Wen, L. Huang, X. Wang and H. Zhang, *J. Power Sources* (2011) In Press.
14. L. Qiu, S. Zhang, L. Zhang, M. Sun and W. Wang, *Electrochim. Acta* 55 (2010) 4632.
15. J. Wang, J. Liu, Z. Ling, J. Yang, C. Wan and C. Jiang, *Electrochim. Acta* 48 (2003) 1861.
16. J. L. Wang, J. Yang, J. Y. Xie, N. X. Xu and Y. Li, *Electrochem. Commun*. 4 (2002) 499.
17. J. Chen, X. Jia, Q. She, C. Wang, Q. Zhang, M. Zheng and Q. Dong, *Electrochim. Acta* 55 (2010) 8062.
18. X. Yu, J. Xie, J. Yang and K. Wang, *J. Power Sources* 132 (2004) 181.
19. H. Karami, O. Rostami-Ostad Kalayeh, *J. Clust. Sci*. 20 (2009) 587.
20. H. Karami, M. Alipour, *J. Power Sources* 191 (2009) 653.
21. H. karami and M. Alipour, *Int. J. Electrochem. Sci*. 5 (2010) 706.